https://doi.org/10.5194/cp-2019-119
Preprint. Discussion started: 7 October 2019

Climate of the Past
Discussions
Open Access

Centennial-scale monsoon changes since the last deglaciation linked to solar activities and North Atlantic cooling

Xingxing Liu[1,*], Youbin Sun[1,*], Jef Vandenberghe[2], Peng Cheng[1], Xu Zhang[3,4], Evan J Gowan[4], Gerrit Lohmann[4], Zhisheng An[1]

[1]State Key Laboratory of Loess and Quaternary Geology, Institute of Earth Environment, Chinese Academy of Sciences, Xi'an 710061, China

[2]Institute of Earth Sciences, Vrije Universiteit, De Boelelaan 1085, 1081 HV Amsterdam, The Netherlands

[3]Key Laboratory of Western China's Environmental Systems (Ministry of Education), College of Earth and Environmental Sciences, Lanzhou University, Lanzhou, 730000, China

[4]Alfred Wegener Institute Helmholtz Centre for Polar and Marine Research, Bussestrasse 24, D-27570 Bremerhaven, Germany

[*]Corresponding author: Xingxing Liu (liuxx@ieecas.cn) and Youbin Sun (sunyb@ieecas.cn)

Abstract

Rapid monsoon changes since the last deglaciation remain poorly constrained due to the scarcity of geological archives. Here we present a high-resolution scanning X-ray fluorescence (XRF) analysis of a 13.5-m terrace succession on the western Chinese Loess Plateau (CLP) to infer rapid monsoon changes since the last deglaciation. Our results indicate that Rb/Sr and Zr/Rb are sensitive indicators of chemical weathering and wind sorting, respectively, which are further linked to the strength of the East Asia summer and winter monsoon. These two parameters exhibit an anti-phase relationship between the summer and winter monsoon changes on

https://doi.org/10.5194/cp-2019-119
Preprint. Discussion started: 7 October 2019

centennial timescale during 16~1 ka BP. Comparison of these monsoon changes with solar activity and North Atlantic cooling events reveals that both factors can lead to abrupt changes on the centennial timescale in the early Holocene. During the late Holocene, North Atlantic cooling became the major forcing of centennial monsoon events.

Keywords: Chinese Loess Plateau; East Asian monsoon; elemental ratios; centennial variability; monsoon dynamics

1 Introduction

The East Asian monsoon (EAM) is one of the most important atmospheric circulation systems linked to climate changes over high- and low-latitude regions of the Northern Hemisphere (Ding, 1994). It consists of summer and winter monsoons (EASM and EAWM) with significantly seasonal changes in moisture transportation and wind direction. During the past three decades, variability of the rain-bearing EASM on millennial to centennial time scales has been investigated extensively from cave deposits (Dykoski et al., 2005; Wang et al., 2005; Cheng et al., 2016), loess sequences (An et al., 1991; Ding et al, 1995; Sun et al., 2006, 2016; Kang et al., 2018), lake sediments (Yancheva et al., 2007; An et al., 2012; Chen et al., 2015; Liu et al., 2016), marine sediments (Huang et al., 2011), and model simulations (Wen et al., 2016). These previous studies show a series of oscillations and/or abrupt events, such as the 4.2, 8.2, 9.2 and 10.3 ka events. These records suggest the summer monsoon variations are not only induced by changes in Northern Hemisphere summer insolation, but also strongly modulated by internal land-ocean-air interactions of the Earth-climate systems (e.g., An et al., 2015).

Unlike abundant proxies of the EASM variability, high-resolution records reflecting millennial to centennial EAWM variability are still sparse. Though various proxies from

https://doi.org/10.5194/cp-2019-119
Preprint. Discussion started: 7 October 2019

different paleoclimatic archives have been used to document EAWM evolution since the last deglaciation, great differences were observed on the inferred winter monsoon changes and forcing mechanisms (Yancheva et al., 2007; Huang et al., 2011; Wang et al., 2012; Li and Morrill, 2015; Kang et al., 2018) . There are four primary factors contribute to these conflicting records. First, the loess-paleosol record on the Chinese Loess Plateau (CLP) (Sun et al., 2012; Kang et al., 2018) or marine sediments from the South China Sea (Huang et al., 2011) are not of sufficiently high resolution to detect centennial EAWM changes due to relatively-low sedimentation rates. Second, the sensitivity of various archives and proxies to changes in the monsoon intensity is different (e.g., Yancheva et al., 2007; Huang et al., 2011; Kang et al., 2018). Some environmental proxies commonly show different amplitudes and timing of variation, likely reflecting the fact that they respond to different aspects of climate and environment (temperature, wind and precipitation). Third, the proxies used for the EAWM remains controversial, such as whether Titanium (Ti) in Huguang Maar Lake is a proxy for local hydrology or EAWM intensity (Yancheva et al., 2007; Zhang et al., 2007). Fourth, uncertain chronologies from diverse natural archives (e.g., loess, lake, and marine) may lead to timing mismatch on centennial timescales.

Wen et al. (2016) performed a set of long-term transient simulations that suggest the EASM and EAWM are anti-correlated on millennial timescales in response to North Atlantic meltwater forcing during the last 21 ka. However, there is still a lack of high-resolution proxies to support this modelling result. This hampers our understanding of the effects of external solar forcing and internal meltwater feedbacks (Li and Morrill, 2015; Wen et al., 2016). Though numerous studies have focused on the rapid climate changes on the EASM and EAWM since the last deglaciation, significant differences and asynchronous changes still exist (e.g., Wang et al., 2005; Yancheva et al., 2007; Huang et al., 2011; An et al., 2012; Chen et al., 2015). Therefore, it

https://doi.org/10.5194/cp-2019-119
Preprint. Discussion started: 7 October 2019

is crucial to investigate high-resolution, independent proxies with robust chronology of the summer and winter monsoon intensities in one single archive to improve our understanding of rapid monsoon changes and dynamics in particular the centennial variability and coherent forcing mechanisms.

In this study, we investigate a thick terrace succession on the western CLP to determine EAWM and EASM variability since the last deglaciation for the first time. Our results provide valuable insights into the relationship between the EAWM and EASM variability at centennial timescales using high-resolution (5-mm interval) elemental records obtained by X-ray fluorescence (XRF) core scanning. We compare the elemental ratios (Zr/Rb and Rb/Sr) with other paleo-records of abrupt monsoon changes to determine the links with external solar forcing and internal feedbacks.

2 Materials and Methods

The Dadiwan section (DDW, 35.02°N, 105.8°E, 1454 m a.s.l) in Qin'an County, Gansu Province is located on the first terrace of the Wei River on the western CLP (Fig. 1A). Fluvio-aeolian sediments are thick and widely deposited on river terraces of the Wei River and its tributaries in this area (Fig. 1B). From 1981 to 2010, the mean annual precipitation and mean annual temperature in Qin'an County is 507.3 mm and 10.4℃, respectively. Dadiwan is known as the oldest example and type site of the "Dadiwan cultural" or "Laoguantai cultural" complex, which is the westernmost expression of early millet agriculture in North China. Previous studies in Dadiwan area based on organic carbon and pollen revealed that the middle Holocene was the most humid interval since the last deglaciation (Feng et al., 2004). During April 2015, we retrieved a 13.5-m core using a hydraulic-static drilling rig with a dual-tube (outer and inner

https://doi.org/10.5194/cp-2019-119
Preprint. Discussion started: 7 October 2019

Climate of the Past Discussions
Open Access
EGU

tubes) core barrel. The core recovery rate was almost 100%, though some cores were slightly compressed (Fig. 1C).

After splitting the cores into a working and archive half with a Geotek core splitter, the surface of the cores was carefully smoothed to reduce scanning errors caused by irregularities from core slicing (Fig. 1C). The split core surface was subsequently covered with a 4 μm Ultralene film during core logging in order to avoid contamination of the XRF detector window and to prevent desiccation of the core surface. The split cores were scanned every 5-mm using an Avaatech XRF core scanner at the Institute of Earth Environment, Chinese Academy of Sciences. The elements measured range from Al to Fe in the periodic table were detected at an X-ray voltage of 10 kV, Co to Mo at 30 kV, and Te to Ba at 50 kV (Richter et al., 2006; Weltje and Tjallingii, 2008). On the basis of the processed model, we used the WinAxil and WinAxilBatch software to calculate the element counts (counts per second, CPS) as peak integrals and applied background subtraction. The quality of every single spectrum and peak integral can be easily checked with the χ^2 value (Van Espen et al., 1977). As the variation in element concentrations of loess can be related to grain size sorting and chemical weathering (Chen et al., 1999, 2006; Peng and Guo, 2001), three elements (Rb, Zr and Sr) with high concentrations and low analytical uncertainties which were detected at 30 kV are discussed in this study.

After core scanning, sub-samples were taken at contiguous 1-cm intervals. A total of 1350 sub-samples were obtained for grain size and magnetic susceptibility analyses (see Fig. 2 in Liu et al., 2018 for a detailed description). A rough chronology of the DDW section was established by acceleratormass spectrometer (AMS) ^{14}C dates based on five total organic carbon from bulk sediments (Liu et al., 2018). In this study, seven additional ^{14}C dates from bulk organic matter were obtained in order to get more reliable age control. The samples were

https://doi.org/10.5194/cp-2019-119
Preprint. Discussion started: 7 October 2019

Climate of the Past
Discussions

pretreated with 1M HCl (2 hr, 60°C) to remove carbonate, and then were thoroughly rinsed with distilled water (Zhou et al., 2006). Pretreated samples and CuO powder were placed into 9-mm quartz tubes, evacuated to 1×10^{-5} Torr, and then combusted. The pure CO_2 was collected using liquid nitrogen and reduced to graphite for AMS dating. For the AMS analysis, the CO_2 was reduced to graphite using Zn/Fe catalytic reduction. All these selected 12 samples were analyzed using a 3MV tandem accelerator at the Xi'an accelerated mass spectroscopy center and calibrated using calib. 7.0.2 (Reimer et al., 2004).

3 Results

Based on soil structure, color, magnetic susceptibility and grain size, the 13.5-m DDW core can be divided lithologically into three sub-units from bottom to top: 13~13.5 m, fluvial sediments; 6~13 m, loess deposits; 0~6 m, paleosol interbedded with four weakly weathered paleosol layers (Fig. 2A). The 12 radiocarbon ages have a linear correlation with depth. This is consistent with a continuous sediment accumulation under a stable environment between 16~1 ka BP. The age-depth model is constructed using linear regression ($y=1.1465x+1.2546$, $R^2=0.9921$) (Fig. 2B). We can resolve centennial-scale monsoon variations since the last deglaciation, due to the dating errors range from 24 to 50 years and the sedimentation rate is high (0.09 cm/yr).

The magnetic susceptibility displays a stepwise increase from $\sim13.7\times10^{-8}m^3kg^{-1}$ below 6 m to $15.5\sim138.6\times10^{-8}m^3kg^{-1}$ above 6 m, with maximum values at three strongly weathered soil layers (Fig. 2C). Mean grain size, however, exhibits a two-stage variability except for the lower 0.5-m fluvial sandy layers (not shown here because it goes off the scale) (Fig. 2D); The lower part (13.5~6 m) exhibits large fluctuations (7.9~121.3 μm) while the loess-paleosol alternations (6~0 m) show small fluctuations (6.4~28.8 μ m). Generally, high magnetic susceptibility

https://doi.org/10.5194/cp-2019-119
Preprint. Discussion started: 7 October 2019

corresponds to fine mean grain-size, but the abrupt MS increase around 6 m is different from the gradual fining of the mean grain size between 8.2~6.8 m.

Similar to variations of magnetic susceptibility and grain-size, Rb, Sr and Zr exhibit significant variability, with ranges of 3400~8827 cps for Rb (Fig. 2E), 7000~40000 cps for Sr (Fig. 2F), and 7000~30000 cps for Zr (Fig. 2G). Low Rb/Sr ratio values correspond to low magnetic susceptibility, with values in the range from 0.18 to 0.6, revealing distinct pedogenic weathering effects. (Fig. 2H). The variation of the Zr/Rb ratio ranges from 1.2 to 5.8. High Zr/Rb ratios occur where grain-size is coarse, suggesting grain-size sorting effects (Fig. 2I).

4 Discussion

4.1 Centennial monsoon variability since the last deglaciation

A number of elements (e.g. Al, Si, K, Ca, Ti, Fe, Mn, Rb, Zr, Sr) based on scanning XRF have been used to acquire information of past climatic and environmental changes (Richter et al., 2006; Liang et al., 2012; Sun et al., 2016). However, the interpretation of lighter elements data require careful consideration due to the instrument detection limits and analytical uncertainties (e.g. organic matter and water content) (Richter et al., 2006). Considering the sedimentary characteristics and geochemical behavior of Zr (commonly abundant in coarse-grained sediments and resistant to weathering), Rb (enriched in clay deposits, relatively stable) and Sr (easily mobilized during chemical weathering), the ratios of Zr/Rb can be an indicator of grain-size sorting and Rb/Sr is an indicator of chemical weathering (Chen et al., 1999, 2006; Peng and Guo, 2001). Previous studies demonstrated that grain size and magnetic susceptibility of loess-paleosol sequences have been widely used as proxies for winter and summer monsoons, respectively (An et al., 1991; Ding et al, 1995; Sun et al., 2006). Taking into account the ratio of

Zr/Rb and Rb/Sr are highly consistent with grain-size and magnetic susceptibility (Fig. 2), we used Zr/Rb and Rb/Sr ratios as proxies for EAWM and EASM intensity, respectively.

The Zr/Rb and Rb/Sr ratios reveal significant centennial- to millennium-scale variability (Fig. 3). During the last deglaciation, the Zr/Rb ratio has large-amplitude, high-frequency fluctuations, in contrast to small-amplitude and low-frequency oscillations during the Holocene (Fig.3B). The Rb/Sr ratio exhibits relatively small-amplitude fluctuations during the last deglaciation to early Holocene (16~9.7 ka BP) and mid-to-late Holocene (7-1 ka BP). In the early to mid-Holocene (9.7-7 ka BP), there are large amplitude fluctuations (Fig. 3C). It reveals a anti-phased relationship between EAWM and EASM on centennial-scale. That is, when the EAWM is strong, the EASM is weak. A series of strong EAWM and weak EASM events (e.g., H1, YD, 11.1, 10.1, 9.3, 8.2, 7.3, 6.7, 5.9, 4.6 and 2.1 ka) can be identified from Zr/ Rb and Rb/Sr values. However, some of the intervals (e.g., YD, 11.1, 6.7 ka) are more distinct in the Zr/Rb ratio, while some intervals such as the 7.3 ka event is more distinct in the Rb/Sr ratio. The differences between the two proxies records during these abrupt intervals shows that they have variable sensitivity to monsoonal wind and precipitation intensity changes (Sun et al., 2012; Chen et al., 2015).

The centennial-scale winter monsoon changes since the last deglaciation reconstructed at DDW are partially consistent with previous high-resolution Ti records from Lake Huguang Maar in southern China (Fig. 3A, Yancheva et al., 2007). This support that the record of Ti counts can be a measure of winter monsoon strength although it is still controversial due to the provenance of the lake sediments (Yancheva et al., 2007; Zhang et al., 2007). Some of the strong winter monsoon intervals (e.g., 7.3 ka) are not significant in the Lake Huguang Maar, which indicate that DDW, located in northern China, is more sensitive to the EAWM system.

https://doi.org/10.5194/cp-2019-119
Preprint. Discussion started: 7 October 2019

Climate of the Past
Discussions
Open Access

Compared with other summer monsoon proxy records in China, the centennial-scale EASM changes at DDW are consistent with the Lake Qinghai summer monsoon index (SMI) (Fig.3D, An et al., 2012) and the ^{18}O record from Dongge Cave stalagmites in eastern China (Fig.3E, Dykoski et al., 2005; Wang et al., 2005). Almost all the weak summer monsoon intervals, within dating errors, appear to coincide with major changes in the ^{18}O record from Dongge Cave. This indicates that Rb/Sr from DDW and ^{18}O record of Dongge Cave both responded to changes in solar output (Wang et al., 2005; Dykoski et al., 2005). There are some discrepancies between DDW and Qinghai Lake, such as the 8.2 ka event, which was not significant in the Qinghai Lake. This could be ascribed to age model discrepancies, or the variable sensitivity of different proxies to changes in monsoon intensity (Chen et al., 2015). Therefore, the other weak EASM intervals existing in three different regions (CLP, northeast of Tibetan Plateau and eastern China) may have recorded centennial EASM variability since the last deglaciation.

4.2 Links between solar forcing and high-latitude climate changes

We removed the long-term trend of Zr/Br and Rb/Sr ratios to investigate the high frequency components of the signal (<1 kyr), then compare the results with the North Atlantic hematite-stained grains records (HSG, Fig. 4A) (Bond et al.,2001) and atmospheric ^{14}C production rate ($\triangle^{14}C$) (Fig. 4D) (Reimer et al., 2013). HSG is a tracer of drift ice in the North Atlantic, high values of HSG indicate cold conditions (Bond et al., 2001). Higher values of atmospheric $\triangle^{14}C$ represent weak solar activity and vice versa (Stuiver and Quay, 1980). High-frequency components of the EAWM and EASM proxies from DDW exhibit large-amplitude fluctuations during the early Holocene (11.5~7 ka), while the amplitude variations were more moderate during the late Holocene (7~1 ka), especially the Rb/Sr ratio (Fig. 4B and C). All the

https://doi.org/10.5194/cp-2019-119
Preprint. Discussion started: 7 October 2019

strong winter and weak summer monsoon intervals from DDW records can either be correlated with HSG (Fig. 4A), or with high atmospheric $\triangle^{14}C$ (Fig. 4D). This indicate possible relationship with Northern Hemisphere cooling and solar activity.

During the early Holocene (11.5~7 ka), all of the strong EAWM/weak EASM intervals (e.g., 11.1, 10.1, 9.3, 8.2, 7.3 ka BP) within the limits of dating error are correlated with HSG and high $\triangle^{14}C$. High similarity of these records suggests that the North Atlantic cooling events and solar activity probably simultaneously affect the EAM systems on centennial timescales. During the late Holocene (7~1 ka), all the strong EAWM and weak EASM events (e.g., 6.7, 5.9, 4.6, 3.3, 2.8 and 2.1 ka BP) correspond well to the abrupt events in the North Atlantic region. This indicates that North Atlantic cooling plays an important role in driving the centennial monsoon changes during the late Holocene. The 3.3 and 2.8 ka events are also correlated well with high $\triangle^{14}C$, which indicate solar forcing also plays a role during those times.

In order to further confirm the possible link of monsoon variability with internal North Atlantic feedbacks and external solar forcing on centennial-scale, spectral analyses were conducted on these proxies for the early (11.5~7 ka) and late (7~1 ka) Holocene (Fig. 4). The spectral results reveal that the Zr/Rb and Rb/Sr records both display a prominent periodicity at 1.0 kyr (Fig. 4F and G). This matches with the cycle of HSG (Fig. 4E) and $\triangle^{14}C$ (Fig. 4H) during the early Holocene. The similarity in periodicity further confirm the link of centennial EAM variability to North Atlantic cooling and solar activities during the early Holocene (11.5~7 ka). However, the dominant periodicity (~1.27 kyr) of HSG, Zr/Br and Rb/Sr records are not evident in the $\triangle^{14}C$ spectrum during the late Holocene (7~1 ka) (Fig.4I-L), implying that solar forcing is not the dominant cause of centennial monsoon variability during this period.

https://doi.org/10.5194/cp-2019-119
Preprint. Discussion started: 7 October 2019

North Atlantic cooling and solar activity are two commonly accepted drivers of centennial climate variability. There is a teleconnection between rapid monsoon changes and abrupt events in the North Atlantic region (the ocean thermohaline circulation) (Broecker et al., 1992; Alley et al., 1997; Bond et al., 2001; Wang et al., 2005). The strength of the Siberian High, located north of our DDW section, increases when the North Atlantic is in a cold mode (Gong et al., 2001). The Intertropical Convergence Zone (ITCZ) shifted southward due to changes in the Atlantic Meridional Overturning Circulation (AMOC) and temperature gradients across the northern hemisphere. When ITCZ shifted southward, the EASM weakened and EAWM strengthened (Broccoli et al., 2006; Sun et al., 2012; Wen et al., 2016). Speleothem records from China (Dykoski et al., 2005; Cheng et al., 2006; Wang et al., 2008) and many model simulations (Chiang and Bitz 2005; Broccoli et al. 2006) support this.

The change in solar activity could contribute to the regional monsoon variability by affecting low-latitude hydrological processes (Liu et al. 2009; Yan et al. 2015). Specifically, decreased summer insolation results in changes to the land-ocean thermal contrast. The sea surface temperature in the western tropical Pacific decreases and the Northwest Pacific Subtropical High weakens (Liu et al., 2003; Cai et al., 2010). This decreased thermal contrast would result in a southward migration of the ITCZ and also weaken the EASM strength by reducing the monsoon moisture transport from the tropical ocean to the continent in low latitudes (Liu et al. 2009; Yan et al. 2015). Since changes in solar output are large at centennial-scale during the early Holocene, this may amplify the solar output effect due to nonlinear responses and feedback processes of the climate system (Mohtadi et al., 2016). During the late Holocene (7~1 ka), there is a decrease of summer insolation and the small-amplitude fluctuations of solar

https://doi.org/10.5194/cp-2019-119
Preprint. Discussion started: 7 October 2019

activities (Fig. 4D) (Berger, 1978). This is probably why it play a less important role in EAM system.

5 Conclusions

We recovered a high-resolution last deglaciation record of EAWM and EASM from terrace sediments on the western CLP. Ratios of Zr/Rb and Rb/Sr are sensitive indicators of winter wind intensity and chemical weathering, respectively, and thus can be regarded as an index of EAWM and EASM. A number of strong and weak monsoon changes are identified by means of Zr/Br and Rb/Sr values from DDW, such as strong EAWM/weak EASM intervals around H1, YD, 11.1, 10.1, 9.3, 8.2, 5.9, 4.6, 3.3, 2.8 and 2.1 ka, which reveals a negative co-variabiltiy between the EAWM and EASM on centennial time scale. Our Zr/Rb and Rb/Sr records are consistent with the Ti content from Lake Huguang Maar (EAWM proxy), the SMI from Lake Qinghai and the ^{18}O record from the Dongge cave (both EASM proxies). Comparing with North Atlantic cooling and solar activity proxies, our record shows that both are possible driving factors of centennial monsoon variability. North Atlantic cooling events and solar activity are the dominant forcing of the EAM system during the early Holocene, while North Atlantic cooling became more important during the late Holocene.

Data availability

All data are accessible from the authors. Correspondence and requests for materials should be addressed to Xingxing Liu (liuxx@ieecas.cn).

Author contributions

Xingxing Liu and Youbin Sun designed the study and performed the fieldwork and experiments. Jef Vandenberghe, Xu Zhang contributed to data analysis. Peng Cheng conducted the AMS 14C analysis. Evan J Gowan, Gerrit Lohmann and Zhisheng An improved the manuscript with their contributions.

Competing interests

The authors declare that they have no conflict of interest.

Acknowledgments

This work was supported by The National Key Research and Development Program of China (2016YFA0601902), the National Science Foundation of China (41807425 and 41525008), and the Open Foundation of State Key Laboratory of Loess and Quaternary Geology (SKLLQG1633).

References

Alley, R.B., Mayewski, P.A., Sowers, T., Stuiver, M., Taylor, K.C., and Clark, P.U.: Holocene climatic instability: A prominent, widespread event 8200 yr ago, Geology, 25 (6), 483-486, 1997.

An, Z.S., Colman, S.M., Zhou, W.J., Li, X.Q., Brown, E.T., Jull, A.J.T., Cai, Y.J., Huang, Y.S., Lu, X.F., Chang, H., Song, Y.G., Sun, Y.B., Xu, H., Liu, W.G., Jin, Z.D., Liu, X.D., Cheng, P., Liu, Y., Ai, L., Li, X.Z., Liu, X.J., Yan, L.B., Shi, Z.G., Wang, X.L., Wu, F., Qiang, X.K., Dong, J.B., Lu, F.Y., and Xu, X.W.: Interplay between the Westerlies and Asian monsoon recorded in Lake Qinghai sediments since 32 ka, Scientific Reports, 2, 619, 2012.

An, Z.S., Kukla, G., Porter, S.C., and Xiao, J.L.: Late Quaternary dust flow on the Chinese loess plateau, Catena, 18 (2), 125-132, 1991

An, Z.S., Wu, G.X., Li, J.P., Sun, Y.B., Liu, Y.M., Zhou, W.J., Cai, Y.J., Duan, A.M., Li, L., Mao, J.Y., Cheng, H., Shi, Z.G., Tan, L.C., Yan, H., Ao, H., Chang, H., and Juan, F.: Global Monsoon Dynamics and Climate Change, Annu. Rev. Annual Review of Earth and Planetary Sciences, 43, 2.1-2.49, 2015.

Berger, A.: Long term variations of daily insolations and quaternary climatic changes, Journal of the Atmospheric Sciences, 35, 2362-2367, 1978.

Berntsson, A., Rosqvist, G.C., and Velle, G.: Late-Holocene temperature and precipitation changes in Vindelfjällen, mid - western Swedish Lapland, inferred from chironomid and geochemical data, The Holocene, 24: 78-92. doi: 10.1177/0959683613512167, 2014.

Bond, G., Kromer, B., Beer, J., Muscheler, R., Evans, M.N., Showers,W., Hoffmann, S., Lotti Bond, R., Hajdas, I., and Bonani, G.: Persistent solar influence on North Atlantic climate during the Holocene, Science, 294 (5549), 2130-2136, 2001.

Broccoli, A. J., Dahl, K. A., and Stouffer, R. J.: Response of the ITCZ to Northern Hemisphere cooling, Geophysical Research Letters, 33(1), 2006.

Broecker, W., Bond, G., Klas, M., Clark, E., and McManus, J.: Origin of the northern Atlantic's Heinrich events, Climate Dynamics, 6 (3-4), 265-273, 1992.

Cai, Y.J., Tan, L.C., Cheng, H., An, Z.S., Edwards, R.L., Kelly, M.J., Kong, X.G.,and Wang, X.F.: The variation of summer monsoon precipitation in Central China since the last deglaciation, Earth and Planetary Science Letters, 291 (1), 21-31, 2010.

Chen, F., Xu, Q., Chen, J., Birks, H.J.B., Liu, J., Zhang, S., Jin, L., An, C., Telford, R.J., Cao, X., Wang, Z., Zhang, X., Selvaraj, K., Lu, H., Li, Y., Zheng, Z., Wang, H., Zhou, A., Dong, G.,

https://doi.org/10.5194/cp-2019-119
Preprint. Discussion started: 7 October 2019

Zhang, J., Huang, X., Bloemendal, J., and Rao, Z.: East Asian summer monsoon precipitation variability since the last deglaciation, Scientific Reports, 5, 11186, 2015.

Chen, J., An, Z.S., Wang, Y.J., Ji, J.F., Chen, Y., and Lu, H.Y.: Distribution of Rb and Sr in the Luochuan loess-paleosal sequence of China during the last 800 kaimplications for paleomonsoon variations, Science China Earth Sciences, 42, 225-232, 1999.

Chen, J., Chen, Y., Liu, L., Ji, J., Balsam, W., Sun, Y., and Lu, H.: Zr/Rb ratio in the Chinese loess sequences and its implication for changes in the East Asian winter monsoon strength, Geochimica et Cosmochimica Acta, 70, 1471-1482, 2006.

Cheng, H., Edwards, R. L., Wang, Y., Kong, X., Ming, Y., Kelly, M. J., Wang, X.F., Gallup, C.D., and Liu, W.G.: A penultimate glacial monsoon record from Hulu Cave and two-phase glacial terminations, Geology, 34(3), 217-220, 2006.

Cheng, H., Edwards, R.L., Sinha, A., Spotl, C., Yi, L., Chen, S.T., Kelly, M., Kathayat, G., Wang, X.F., Li, X.L., Kong, X.G.,Wang, Y.J., Ning, Y.F., and Zhang, H.W.: The Asian monsoon over the past 640,000 years and ice age terminations, Nature, 534, 640-646, 2016.

Chiang, J.C.H., and Bitz, C.M.: Influence of high latitude ice cover on the marine Intertropical Convergence Zone, Climate Dynamics, 25, 477-496, 2005.

Ding, Y.H.: Monsoon over China, Kluwer Academic, p. 420, 1994.

Ding, Z.L., Liu, T.S., Rutter, N.W., Yu, Z.W., Guo, Z.T., and Zhu, R.X.: Ice-volume forcing of East Asian winter monsoon variations in the past 800,000 years, Quaternary Research, 44 (2), 149-159, 1995.

Dykoski, C.A., Edwards, R.L., Cheng, H., Yuan, D.X., Cai, Y.J., Zhang, M.L., Liu, Y.S., Qing, J.M., An, Z.S., and Revenaugh, J.: A high-resolution, absolute-dated Holocene and

https://doi.org/10.5194/cp-2019-119
Preprint. Discussion started: 7 October 2019

deglacial Asian monsoon record from Dongge cave, China. Earth and Planetary Science Letters, 233 (1), 71-86, 2005.

Feng, Z.D., An, C.B., Tang, L.Y., and Jull, A.J.T.: Stratigraphic evidence of a Megahumid climate between 10,000 and 4000 years BP in the western part of the Chinese Loess Plateau, Global and Planetary Change, 43 (3), 145-155, 2004.

Gong, D.Y., Wang, S.W., and Zhu, J.H.: East Asian winter monsoon and Arctic Oscillation, Geophysical Research Letters, 28 (10), 2073-2076, 2001.

Huang, E., Tian, J., and Steinke, S.: Millennial-scale dynamics of the winter cold tongue in the southern South China Sea over the past 26 ka and the East Asian winter monsoon, Quaternary Research, 75 (1), 196-204, 2011.

Kang, S.G., Wang, X.L., Roberts, H. M., Duller, G. A., Cheng, P., Lu, Y.C., and An, Z.S.: Late Holocene anti-phase change in the East Asian summer and winter monsoons, Quaternary Science Reviews, 188, 28-36, 2018.

Li, Y., and Morrill, C.: A Holocene East Asian winter monsoon record at the southern edge of the Gobi Desert and its comparison with a transient simulation, Climate Dynamics, 45, 1219-1234, 2015.

Liang, L.J., Sun, Y.B., Yao, Z.Q., Liu, Y.G., and Wu, F.: Evaluation of high-resolution elemental analyses of Chinese loess deposits measured by X-ray fluorescence core scanner, Catena, 92: 75-82, 2012.

Liu, J., Wang, B., Ding, Q., Kuang, X., Soon, W., and Zorita, E.: Centennial variations of the global monsoon precipitation in the last millennium: results from ECHO-G model, Journal of Climate, 22:2356-2371, 2009.

https://doi.org/10.5194/cp-2019-119
Preprint. Discussion started: 7 October 2019

Liu, X.X., Sun, Y.B., Vandenberghe, J., Li, Y., and An, Z.: Palaeoenvironmental implication of grain-size compositions of terrace deposits on the western Chinese Loess Plateau, Aeolian Research, 32, 202-209, 2018.

Liu, X.X., Vandenberghe, J., An, Z.S., Li, Y., Jin, Z.D., Dong, J.B., and Sun, Y.B.: Grain size of Lake Qinghai sediments: implications for riverine input and Holocene monsoon variability, Palaeogeography, Palaeoclimatology, Palaeoecology, 449, 41-51, 2016.

Liu, Z., Otto-Bliesner, B., Kutzbach, J., Li, L., and Shields, C.: Coupled climate simulation of the evolution of global monsoons in the Holocene, Journal of Climate, 16 (15), 2472-2490, 2003.

Mohtadi, M., Prange, M., and Steinke, S.: Palaeoclimatic insights into forcing and response of monsoon rainfall, Nature, 533, 191-199, 2016.

Peng, S.Z., and Guo, Z.T.: Geochemical indicator of original eolian grain size and implications on winter monsoon evolution, Science in China Series D: Earth Sciences, 44: 261-266, 2001.

Rasmussen, S.O., Andersen, K.K., Svensson, A.M., Steffensen, J.P., Vinther, B.M., Clausen, H.B., Siggaard-Andersen, M.L., Johnsen, S.J., Larsen, L.B., Dahl-Jensen, D., Bigler, M., Röhlisberger, R., Fischer, H., Goto-Azuma, K., Hansson, M.E., and Ruth, U.: A new Greenland ice core chronology for the last glacial termination, Journal of Geophysical Research: Atmospheres, 111(D6), 2006.

Reimer, P.J., Baillie, M.G.L., Bard, E., Bayliss, A., Beck, J.W., Bertrand, C.J.H., Blackwell, P.G., Buck, C.E., Burr, G.S., Cutler, K.B., Damon, P.E., Edwards, R.L., Fairbanks, R.G., Friedrich, M., Guilderson, T.P., Hogg, A.G., Hughen, K.A., Kromer, B., McCormac, G., Manning, S., Ramsey, C.B., Reimer, R.W., Remmele, S., Southon, J.R., Stuiver, M.,

https://doi.org/10.5194/cp-2019-119
Preprint. Discussion started: 7 October 2019

Talamo, S., Taylor, F.W., van der Plicht, J., and Weyhenmeyer, C.E.: IntCal04 terrestrial radiocarbon age calibration, 0-26 cal kyr BP, Radiocarbon, 46 (3), 1029-1058, 2004.

Reimer, P.J., Bard, E., Bayliss, A., Beck, J.W., Blackwell, P.G., Bronk Ramsey, C., Buck, C.E., Cheng, H., Edwards, R.L., and Friedrich, M.: IntCal13 and Marine13 radiocarbon age calibration curves 0-50,000 years cal BP, Radiocarbon, 55, 1869-1887, 2013.

Richter, T. O., Van der Gaast, S., Koster, B., Vaars, A., Gieles, R., de Stigter, H. C., Haas, H.D., and van Weering, T. C.: The Avaatech XRF Core Scanner: technical description and applications to NE Atlantic sediments, Geological Society, London, Special Publications, 267(1), 39-50, 2006.

Shala, S., Helmens, K., Jansson, K., Kylander, M., Risberg, J., and Lowemark, L.: Palaeoenvironmental record of glacial lake evolution during the early Holocene at Sokli, NE Finland, Boreas, 43: 362-376. doi: 10.1111/bor.12043, 2014.

Stuiver, M., and Quay, P.D.: Changes in atmospheric carbon-14 attributed to a variable sun, Science, 207 (4426), 11-19, 1980.

Sun, Y.B., Chen, J., Clemens, S.C., Liu, Q.S., Ji, J.F., and Tada, R.: East Asian monsoon variability over the last seven glacial cycles recorded by a loess sequence from the northwestern Chinese Loess Plateau, Geochemistry, Geophysics, Geosystems, 7 (12), 2006.

Sun, Y.B., Clemens, S.C., Morrill, C., Lin, X.P., Wang, X.L., and An, Z.S.: Influence of Atlantic meridional overturning circulation on the East Asian winter monsoon, Nature Geoscience, 5 (1), 46-49, 2012.

https://doi.org/10.5194/cp-2019-119
Preprint. Discussion started: 7 October 2019

Climate of the Past
Discussions
Open Access

Sun, Y.B., Liang, L.J., Bloemendal, J., Li, Y., Wu, F., Yao, Z.Q., and Liu, Y.G.: High-resolution scanning XRF investigation of Chinese loess and its implications for millennial - scale monsoon variability, Journal of Quaternary Science, 31(3), 191-202, 2016.

Van Espen, P., Nullens, H., and Adams, F.: A computer analysis of X-ray fluorescence spectra, Nuclear Instruments and Methods, 142(1-2), 243-250, 1977.

Wang, L., Li, J.J., Lu, H.Y., Gu, Z.Y., Rioual, P., Hao, Q.Z., Mackay, A.W., Jiang, W.Y., Cai, B.G., Xu, B., Han, J.T., and Chu, G.Q.: The East Asian winter monsoon over the last 15,000 years: its links to high-latitudes and tropical climate systems and complex correlation to the summer monsoon, Quaternary Science Reviews, 32, 131-142, 2012.

Wang, Y.J., Cheng, H., Edwards, R.L., He, Y., Kong, X., An, Z.S., Wu, J., Kelly, M.J., Dykoski, C.A., and Li, X.: The Holocene Asian monsoon: links to solar changes and North Atlantic climate, Science, 308, 854-857, 2005.

Weltje, G. J., and Tjallingii, R.: Calibration of XRF core scanners for quantitative geochemical logging of sediment cores: theory and application, Earth and Planetary Science Letters, 274(3-4), 423-438, 2008.

Wen, X.Y., Liu, Z.Y., Wang, S.W., Cheng, J., and Zhu, J.: Correlation and anticorrelation of the East Asian summer and winter monsoons during the last 21,000 years, Nature Communications, 7, 11999, 2016.

Yan, H., Soon,W., and Wang, Y.: A composite sea surface temperature record of the northern South China Sea for the past 2500 years: a unique look into seasonality and seasonal climate changes during warm and cold periods, Earth-Science Reviews, 141, 122-135, 2015.

https://doi.org/10.5194/cp-2019-119
Preprint. Discussion started: 7 October 2019

Climate of the Past
Discussions

Yancheva, G., Nowaczyk, N.R., Mingram, J., Dulski, P., Schettler, G., Negendank, J.F.W., Liu, J., Sigman, D.M., Peterson, L.C., and Haug, G.H.: Influence of the intertropical convergence zone on the East Asian monsoon, Nature, 445, 74-77, 2007.

Zhang, D. E., and Lu, L.: Anti-correlation of summer/winter monsoons?. Nature, 450(7168), E7, 2007.

Zhou, W.J., Zhao, X.L., Lu, X.F., Liu, L., Wu, Z.K., Cheng, P., Zhao, W.N., and Huang, C.H.: The 3MV multi-element AMS in Xi'an, China: unique features and preliminary tests, Radiocarbon, 48(2), 285-293, 2006.

https://doi.org/10.5194/cp-2019-119
Preprint. Discussion started: 7 October 2019

Figures

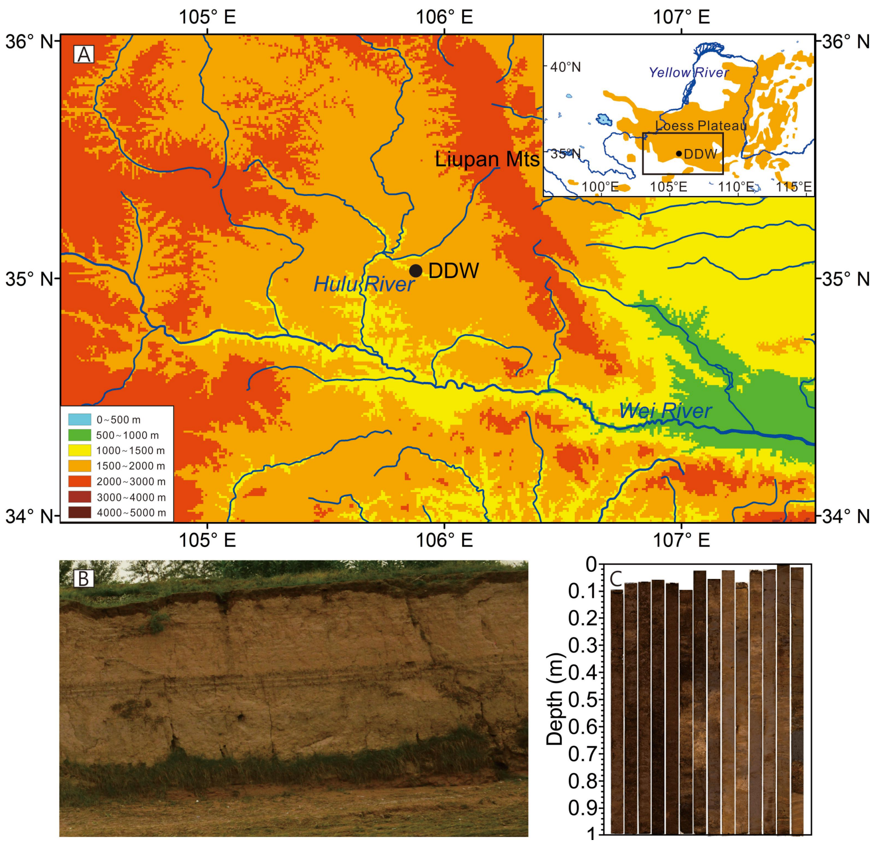

Fig 1. Map showing the CLP and location of the DDW (A), photographs of DDW terrace outcrop (B) and cores (C).

https://doi.org/10.5194/cp-2019-119
Preprint. Discussion started: 7 October 2019

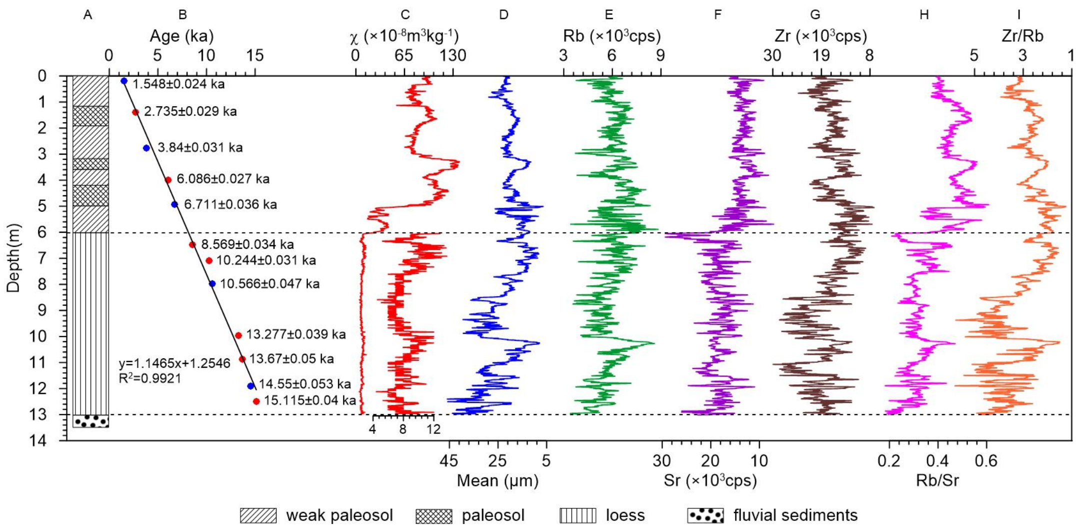

Fig 2. Stratigraphy (A), age-depth model (B), magnetic susceptibility (C), grain-size results (D) and elemental results (E, F, G, H, I) measured by scanning XRF of the DDW core. Five red dots are ages in previous work (Liu et al., 2018). Blue dots are seven additional ages in this study. The elemental results were smoothed with a 3-point moving average.

https://doi.org/10.5194/cp-2019-119
Preprint. Discussion started: 7 October 2019

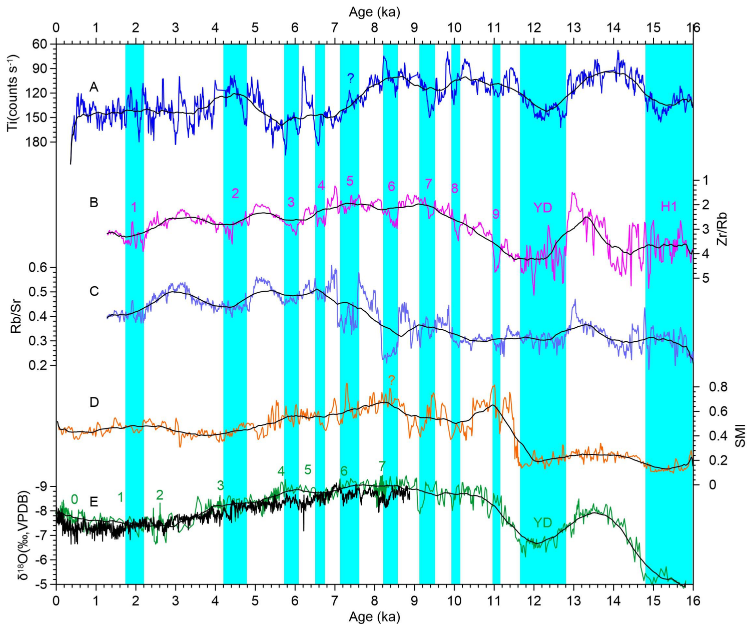

Fig 3. Comparisons of DDW records and other paleoclimatic records. (A) Ti content of Lake Huguang Maar (Yancheva et al., 2007); (B) Zr/Rb of DDW core; (C) Rb/Sr of DDW core; (D) Lake Qinghai summer monsoon index (SMI) (An et al., 2012); (E) Speleothem $\delta^{18}O$ from Dongge Cave (Dykoski et al., 2005; Wang et al., 2005). The cyan bars indicate the timing of abrupt monsoon events in different records.

https://doi.org/10.5194/cp-2019-119
Preprint. Discussion started: 7 October 2019

Climate of the Past
Discussions

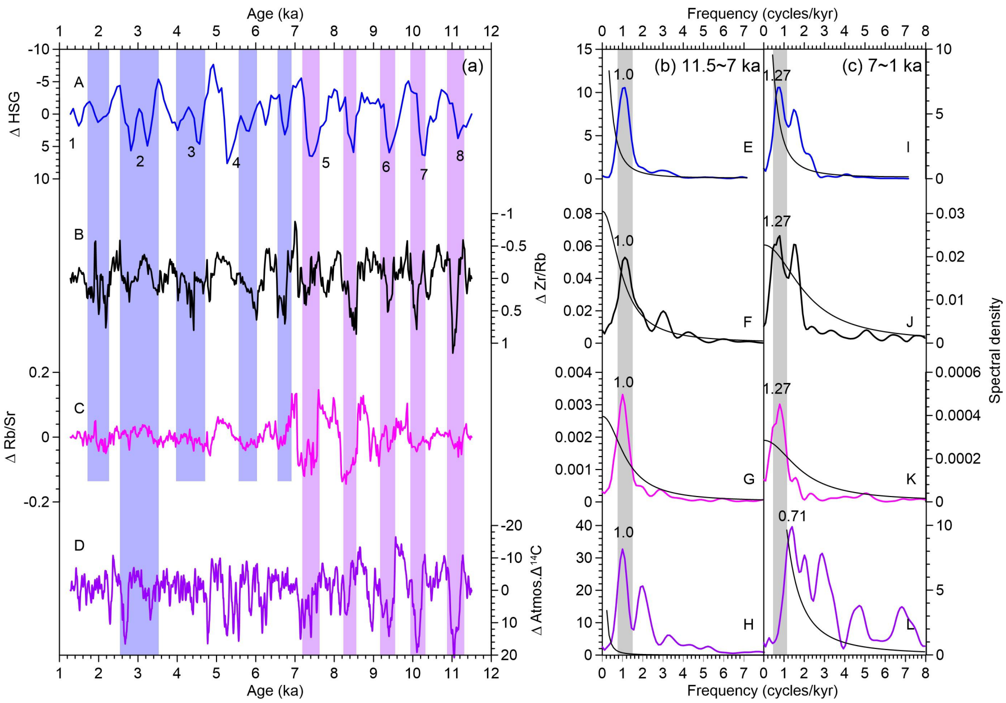

Fig 4. Centennial components (a) of Zr/Rb (B) and Rb/Sr (C) with the North Atlantic HSG (Bond et al., 2001) (A) and atmosphere △^{14}C record (Reimer et al., 2013) (D). The purple and blue bars indicate abrupt monsoon events. The right panel shows the spectra of the proxy records during the early (b) and late Holocene (c). Spectral peaks that are above the 80% confidence levels (black lines) are marked. The grey vertical bands indicate the most significant cycle.